Open access • Journal Article • DOI:10.1109/LAWP.2013.2259211

Dual-Band Suspended-Plate Wearable Textile Antenna — Source link

Nurul Husna Mohd Rais, Ping Jack Soh, Mohd Fareq Abdul Malek, Guy A. E. Vandenbosch

Institutions: Universiti Malaysia Perlis, Katholieke Universiteit Leuven

Published on: 23 Apr 2013 - IEEE Antennas and Wireless Propagation Letters (Institute of Electrical and Electronics Engineers (IEEE))

Topics: Ground plane, Antenna (radio), Directional antenna, Conformal antenna and HiperLAN

Dual-band Suspended-plate Wearable Textile Antenna

Nurul Husna Mohd Rais, Ping Jack Soh, *Student Member, IEEE*, Mohd Fareq Abdul Malek, *Member, IEEE*, and Guy A. E. Vandenbosch, *Fellow, IEEE*

***Abstract*— A novel, dual-band wearable textile antenna fabricated using conductive textiles for operation in both ISM and HiperLAN applications is presented. Its concept is based on the suspended plate antenna. It features a 60×45 mm^2 rectangular radiating element suspended over a 80×60 mm^2 ground plane using a 5 mm foam substrate. The proposed rectangular radiator is modified using slots, slits, and shorting posts to enable dual-band resonance and broad bandwidths in both frequency bands: 277 MHz (2.22 to 2.48 GHz) in the ISM and 850 MHz (4.95 to 5.80 GHz) in the HiperLAN band. The antenna radiates uni-directionally and the ground plane avoids coupling to the users' body. The SP-WTA shows a total efficiency between 67 % and 89 % and a peak gain of 8.33 dB.**

***Index Terms*— Conformal antennas, dual-band antennas, textile antennas, biological effects of electromagnetic radiation.**

I. Introduction

Recently, several investigations have reported on the suspended plate antenna concept [1-3], featuring broadband and ultra wideband (UWB) behaviors. Typically, a suspended-plate antenna (SPA) is a type of shaped microstrip antenna, consisting of a radiator suspended over a ground plane, sandwiched by either air or low permittivity materials with a thickness of ca. 0.1 λ [3]. This low-profile is suitable for wearable applications, as typical textile materials, e.g. foams and fleece are low in permittivity, flexible, are readily available on emergency rescue clothing, and may thus serve as potential substrates. They enable the integration of flexible, robust conductive textiles to form the radiator and ground plane. Textile antennas already have been successfully implemented with satisfactory performance [4-14]. They feature either commercial conductive textiles [4-8], flexible metallic foils [9-10] or metal-coated fibers [12]. Efforts have also been channeled to introduce more attractive features for the wireless on-body communication domain, e.g. the multiple-input multiple-output (MIMO) capability [8] and direction of arrival (DoA) feature [11], besides reducing back radiation using flexible bandgap and waveguide structures [13-14]. Multi-layered or double-sided topologies add to design complexity and are mechanically-prone to degradation due to misalignment, wrinkling, etc.. This topology enables similar flexibility using a single substrate layer, with a much improved bandwidth in each band for on-body detuning mitigation, without the need to sacrifice antenna compactness. To our best knowledge, this is the first dual-band, suspended-plate antenna implemented fully using textiles, including vias. Enhanced using a combination of slots, slits, and via structures, the measured bandwidth achieved in each band (i.e. 12 % and 16 %, respectively) is significantly improved relative to conventional non-UWB suspended-plate antennas [2-3] and wearable dual-band antennas [9-10, 12,14].

Manuscript received February 26, 2013. This work was supported in part by the Malaysian Ministry of Higher Education (MOHE).

H. M. R. Nurul, and P. J. Soh are with the School of Computer and Communication Engineering, Universiti Malaysia Perlis, 02600 Arau, Perlis, Malaysia. H. M. R. Nurul is also with Universiti Kuala Lumpur British Malaysian Institute (UniKL BMI), 53100 Gombak, Selangor, Malaysia.

P. J. Soh and G. A. E Vandenbosch are with KU Leuven, Div. ESAT-TELEMIC, Dept. of Electrical Engineering, Kasteelpark Arenberg 10, 3001 Leuven, Belgium. (phone: +32-(0)16-32-1150; fax: +32-(0)16-32-1986; e-mail: pingjack.soh@esat.kuleuven.be).

M. F. A. Malek is with the School of Electrical Systems Engineering, Universiti Malaysia Perlis, 02600 Arau, Perlis, Malaysia.

II. Antenna Design

The initial topology consists of a rectangular radiator, $L_p \times W_p$, centered above a ground plane, $L_g \times W_g$, as shown in Fig. 1. ShieldIt conductive textile, with 0.17 mm thickness is used as the conductive material. It features 0.03 Ω/sq average surface resistivity (R_s), which translates into a calculated surface conductivity σ_s, of 1.96 x 10^5 S/m. A polyurethane foam substrate (ε_r = 1.07) with thickness h of 5 mm is sandwiched between the radiator and ground plane.

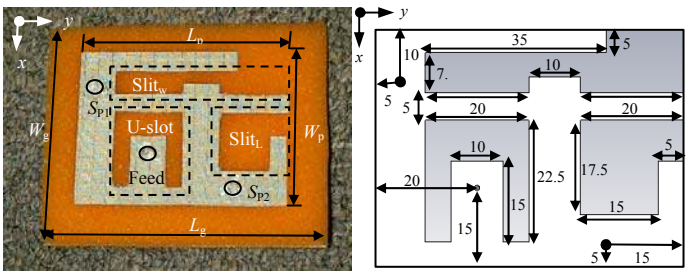

Fig. 1 (a) Fabricated prototype and locations of the U-slot, slits ($Slit_L$, $Slit_W$) and shorting posts (S_{P1} and S_{P2}) on the radiator; (b) detailed radiator dimensions with L_p = 60 mm, W_p = 45 mm, L_g = 100 mm and W_g = 80 mm.

To cover Band 1 (B1), i.e. the ISM (Industrial, Science and Medical) band, the radiator was initially designed to resonate at 2.45 GHz. Aiming at broader bandwidths (BW) its h was first estimated using the technique of [16], yielding 5.8 mm.

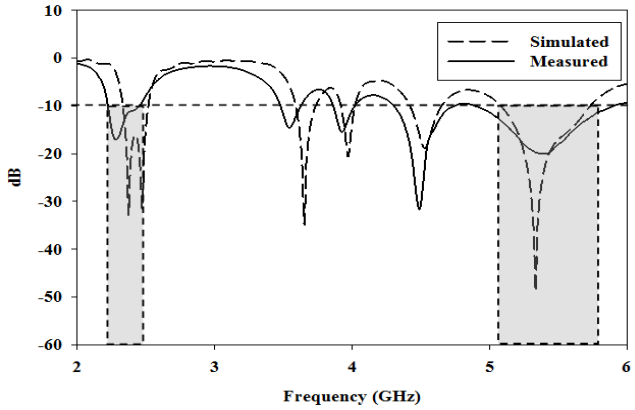

Fig. 2. Simulated and measured reflection coefficients (S_{11}).

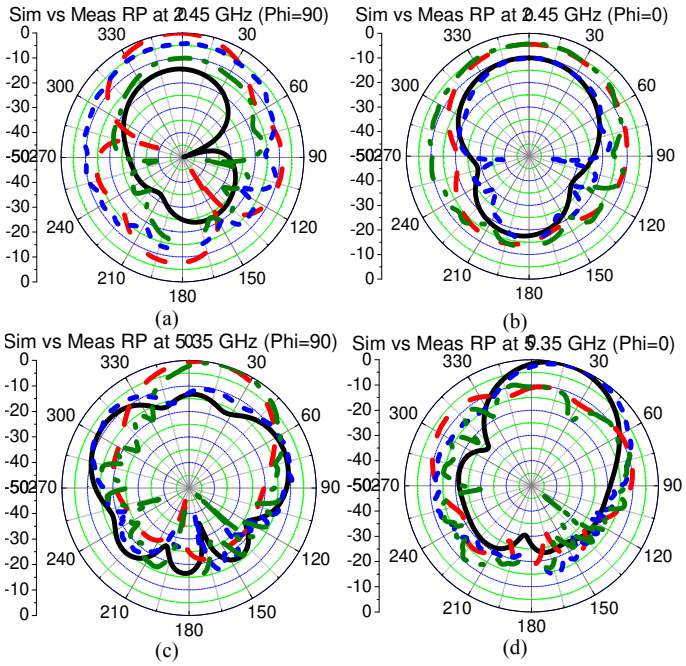

Fig. 3. Simulated and measured radiation patterns for (a) φ=90° cut at 2.45 GHz, (b) φ=0° cut at 2.45 GHz, (c) φ=90° cut at 5.35 GHz, (d) φ=0° cut at 5.35 GHz. Legend: (**black**-solid) = simulated E_φ; (**red**-dashed) = simulated E_θ; (**blue**-short-dash) = measured E_φ; (**green**-dash-dot) = measured E_θ.

In a second step, several modifications are applied to the initial topology. A U-shaped slot is introduced around the feed point to facilitate BW broadening [17], and to allow cancellation of probe inductance. I- and L-shaped slits ($Slit_W$ and $Slit_L$) are integrated into the patch to alter the current paths along its width. Finally, two shorting posts are utilized to generate Band 2 (B2), i.e. 5.15-5.75 GHz HiperLAN (High-Performance Radio LAN). The full topology optimized using CST Microwave Studio is depicted in Fig. 1, with an optimized h of 5 mm. The radiator is fabricated using manual cutting tools, while a conductive epoxy enabled fabric-to-SMA connection. ShieldIt is secured onto the substrate by its adhesive reverse side, while shorting posts S_{P1} and S_{P2} are constructed using conductive threads.

III. Results and Discussion

As can be seen in Fig. 2, simulated and measured reflection coefficients (S_{11}) agree satisfactorily. The B1 BW is 167 MHz (from 2.33 to 2.50 GHz) while B2 features a 700 MHz BW (from 5.05 to 5.75 GHz). Measurements indicate that B1 and B2 span a range from 2.22 to 2.48 GHz, and 4.95 to 5.80 GHz, respectively. A BW increase is observed w.r.t. simulations: 110 MHz and 150 MHz in B1 and B2. The larger B2 BW is also caused by slight fabrication inaccuracies, which affect high frequency performance more severely [5-6].

Radiation patterns are evaluated at the centers of B1 and B2, i.e. at fc_{B1} = 2.45 GHz and fc_{B2} = 5.35 GHz using an anechoic chamber. Calculations agree well with measurements, with its main radiation away from the body, see Fig. 3. This antenna property is expected to avoid high levels of body coupling and absorption. This guarantees a low Specific Absorption Rate (SAR), besides immunity against detuning, as will be presented in the next section. Simulations indicate antenna free space gains of 5.31 dB and 9.34 dB, while measured gains are 3.38 dB and 8.33 dB at 2.45 GHz and 5.35 GHz, respectively. The total efficiency is simulated as 70 % and 92 % while measurements produced decreased efficiencies of 67% and 89 %.

IV. Bending and On-Body Evaluations

To validate the on-body performance, simulations with the antennas placed on the chest and back of a Hugo voxel model were performed. The antennas are spaced 4 mm from the truncated body model to reduce computational resources. A similar setup was utilized during measurement on a male human volunteer (1.78 m, 88 kg). Both antenna mounting locations are shown in Fig. 4, while their simulated and measured S_{11} are illustrated in Fig. 5. Simulations show a constant BW of ca. 180 MHz and 700 MHz in B1 and B2, respectively. Measurements validate this finding, indicating a satisfactory on-body performance. S_{11} variations are due to scattering and absorption by the lossy body area where the antenna is mounted, thus altering impedance matching and detuning the resonance band. However, more severe degradation is avoided due to the presence of the ground plane. SAR simulations on this model further validate this fact. A SAR of 0.14 W/kg is seen on the chest, and 0.24 W/kg on the back, averaged over 10g of tissue, which is well below the ETSI limit of 2 W/kg [15].

The peformance under bent conditions was also investigated. CST MWS was used to simulate SP-WTAs wrapped onto cylinders with radii r of 40, 50, 60, and 70 mm. This radius variation produces different antenna curvatures. They are chosen according to typical human arm sizes. Meanwhile, polystyrene cylinders of corresponding radii were utilized for measurements. The antenna is studied for two bending directions: E- and H-plane, illustrated in Fig. 6(a) and (b), respectively.

Fig. 7(a) presents the simulated S_{11} for different bending radii along the E-plane. No significant changes for B1 are observed: bandwidths are maintained at ca. 190 MHz. For B2, a slight upwards shift is observed as the r is decreased.

However, all changes are insiginificant, except for r = 40 mm when the extreme bending starts to affect the current distribution, and thus, the resonant length.

These main trends are also observed in the measurements shown in Fig. 7(b). Since the B2 resonance generation is dependent on the current length around the U-slot, changes to S_{11} during E-plane bending is unavoidable. Measurements indicate a small downwards resonance shift for B1 when r is decreased.

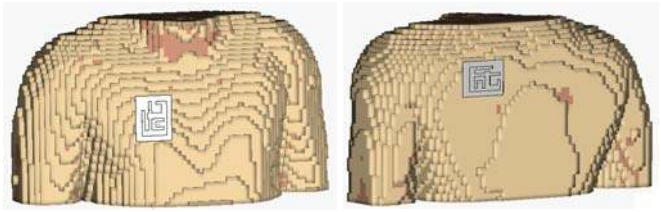

(a) (b)

Fig. 4. On-body antenna mounting locations: (a) chest and (b) back.

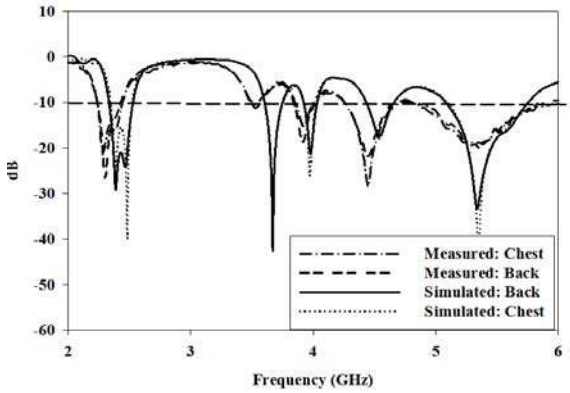

Fig. 5. Simulated and measured S_{11} for different body mounting locations.

(a) (b)

Fig. 6. Antennas bent around cylinders for different directions: (a) E-plane direction and (b) H-plane direction.

Despite best efforts, discrepancies between simulations and measurements still exist. This is caused by the antenna misalignments and different topology in practice, which is unavoidable, since it is impossible to reach a specific bending in the measurements as accurately as in the simulations. Moreover, the foam's ε_r characterized at B1 resulted in a larger simulation-measurement difference at B2 during bending, as was also seen in free space evaluations.

Simulated and measured S_{11} for bending in the H-plane direction for different r are illustrated in Fig. 8. Simulated results in both B1 and B2 with a varying r depicted in Fig. 8(a) show consistency, with minimal bandwidth changes. Fig. 8(b) shows the measured S_{11} for different r in the H-plane direction. Bending the antenna using r = 40, 50, and 60 mm produces a similar fc_{B1} at 2.55 GHz. In contrast, bending using r = 70 mm results in a downward fc_{B1} shift to 2.36 GHz. All measurements in B2 successfully yield a wide impedance bandwidth for all r.

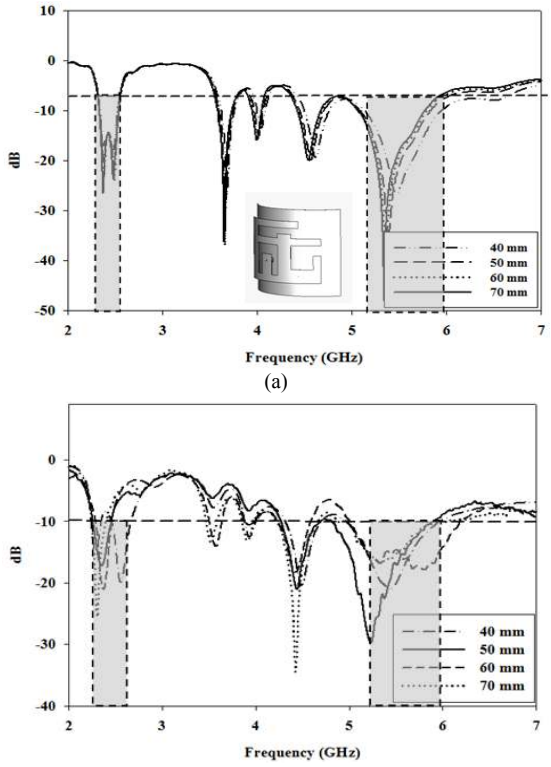

(a)

(b)

Fig. 7. S_{11} for different bending radius at the E-plane direction; (a) simulations, and (b) measurements.

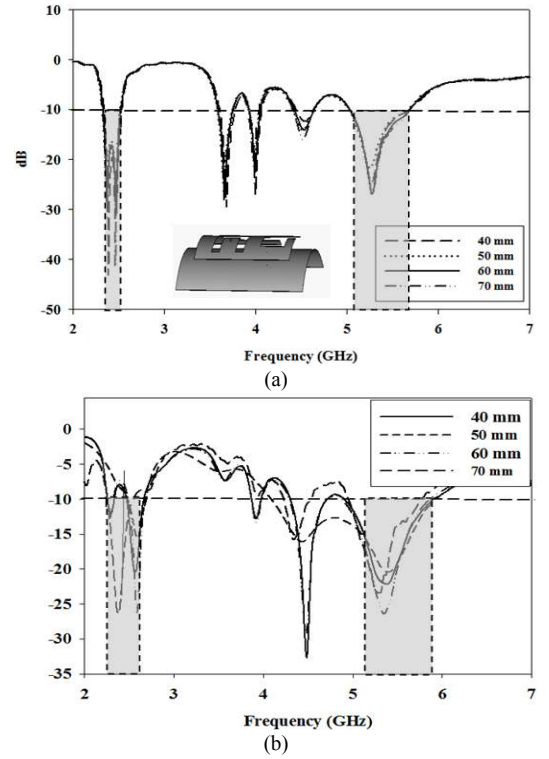

(a)

(b)

Fig. 8. S_{11} for different bending radius at the H-plane direction; (a) simulations, and (b) measurements.

Table 1 summarizes the resonant frequencies and bandwidths for bending in E- and H-plane directions. It is shown that bending in the H-plane direction, which is also along the antenna's width and non-radiating edge, is less effective in changing its reflection performance compared to bending in the E-plane, i.e. along the antenna length.

TABLE I
SIMULATED AND MEASURED BANDWIDTHS (BW) FOR ANTENNA BENDING WITH DIFFERENT RADII AT E-PLANE AND H-PLANE DIRECTIONS

Band/ Bend Direction	*r* (mm)	Sim. Band (GHz)	Sim. BW (GHz)	Meas. Band (GHz)	Meas. BW (GHz)
B1 (E-plane)	40	2.337-2.525	0.188	2.226-2.457	0.231
	50	2.331-2.528	0.197	2.225-2.452	0.227
	60	2.341-2.536	0.195	2.287-2.462	0.175
	70	2.335-2.532	0.197	2.225-2.384	0.159
B1 (H-plane)	40	2.348-2.547	0.199	2.415-2.620	0.205
	50	2.346-2.548	0.202	2.422-2.570	0.148
	60	2.343-2.544	0.201	2.424-2.572	0.148
	70	2.345-2.546	0.201	2.253-2.458	0.205
B2 (E-plane)	40	5.144-5.940	0.796	5.028-5.633	0.605
	50	5.064-5.773	0.709	4.986-5.715	0.729
	60	5.083-5.842	0.759	5.018-6.181	1.163
	70	5.072-5.973	0.901	5.012-5.720	0.708
B2 (H-plane)	40	5.044-5.771	0.727	4.642-5.896	1.254
	50	5.042-5.762	0.720	4.853-5.922	1.069
	60	5.018-5.758	0.740	4.251-5.844	1.593
	70	5.041-5.768	0.727	4.933-5.842	0.909

V. CONCLUSION

A novel, dual-band wearable textile antenna based on the suspended plate concept is proposed and discussed. Systematic patch modification using slots, slits and shorting posts resulted in a dual-band characteristic with satisfactory measured bandwidths of 280 MHz and 850 MHz for ISM and HiperLAN, respectively. The SP-WTA properties - maximum radiation in a direction normal to the radiator with reasonable gains at both frequencies, plus a large ground plane to minimize electromagnetic coupling to the body - are extremely attractive features for wearable applications.

REFERENCES

[1] X. N. Low, Z. N. Chen, W. K. Toh, "Ultrawideband Suspended Plate Antenna with Enhanced Bandwidth and Radiation Performance," *IEEE Trans. on Antennas and Propagation*, vol. 56, no. 8, pp. 2490-2495, Aug. 2008.

[2] Z. N. Chen, "Suspended Plate Antennas with Shorting Strips and Slots," *IEEE Trans. on Antennas and Propagation*, vol. 52, no. 10, pp. 2524-2531, Oct. 2004.

[3] Z. N. Chen, M. Y. M. Chia, "A Novel Center-slot-fed Suspended Plate Antenna," *IEEE Trans. on Antennas and Propagation*, vol. 51, no. 6, pp. 1407-1410, June 2003.

[4] P. J. Soh, G. A. E. Vandenbosch, S. L. Ooi, N. H. M. Rais, "Design of a Broadband All-textile Slotted PIFA," *IEEE Trans. on Antennas and Propagation*, vol. 60, no. 1, pp. 379-384, Jan. 2012.

[5] P. J. Soh, G. A. E. Vandenbosch, S. L. Ooi, M. R. N. Husna, "Wearable dual band Sierpinski fractal PIFA using conductive fabric," *Electronics Letters*, vol. 47, no. 6, pp. 365-367, 2011.

[6] P. J. Soh, S. J. Boyes, G. A. E. Vandenbosch, Y. Huang, S. L. Ooi, "On-body Characterization of Dual-band All-textile PIFAs," *Prog. in Electromagnetics Research*, vol. 129, pp. 517-539, Jul. 2012.

[7] L. Vallozzi, H. Rogier, C. Hertleer, "Dual Polarized Textile Patch Antenna for Integration into Protective Garments," *IEEE Antennas and Wireless Propagation Letters*, vol. 7, pp. 440-443, May 2008.

[8] P. Van Torre, L. Vallozzi, C. Hertleer, H. Rogier, M. Moeneclaey, J. Verhaevert, "Indoor Off-Body Wireless MIMO Communication with Dual Polarized Textile Antennas," *IEEE Trans. on Antennas and Propagation*, vol. 59, no. 2, pp. 631-642, Feb. 2011.

[9] P. Salonen, Y. Rahmat-Samii, H. Hurme, M. Kivikoski, "Dual-band Wearable Textile Antenna," *IEEE Antennas and Propagation Society International Symposium*, 20-25 June 2004, pp. 463-466.

[10] P. Salonen, J. Kim, Y. Rahmat-Samii, "Dual-band E-shaped Patch Wearable Textile Antenna," *IEEE Antennas and Propagation Society International Symposium*, vol. 1A, 3-8 July 2005, pp. 466- 469.

[11] P. J. Soh, B. van den Bergh, H. Xu, H. Aliakbarian, S. Farsi, P. Samal, G. A. E Vandenbosch, D. M. M.-P. Schreurs, B. K. J. C. Nauwelaers, "A Smart Wearable Textile Antenna System for Biomedical Telemetry System," *IEEE Trans. on Microwave Theory and Techniques,* accepted, to be published.

[12] E. K. Kaivanto, M. Berg, E. Salonen, P. de Maagt, "Wearable Circularly Polarized Antenna for Personal Satellite Communication and Navigation," *IEEE Trans. on Antennas and Propagation*, vol. 59, no. 12, pp. 4490-4496, Dec. 2011.

[13] R. Moro, S. Agneessens, H. Rogier, M. Bozzi, "Wearable Textile Antenna in Substrate Integrated Waveguide Technology," *Electronics Letters* , vol. 48, no. 16, pp. 985-987, Aug. 2012.

[14] S. Zhu, R. Langley, "Dual-Band Wearable Textile Antenna on an EBG Substrate," *IEEE Trans. on Antennas and Propagation*, vol. 57, no. 4, pp. 926-935, April 2009.

[15] *Human Exposure to Radio Frequency Fields from Hand-held and Body-mounted Wireless Communication Devices - Human Models, Instrumentation and Procedures*, IEC Standard 62209, 2010.

[16] R. L. Li, G. DeJean, M. M. Tenzeris, J. Laskar, "Integration of Miniaturized Patch Antennas with High Dielectric-constant Multilayer Packages and Soft-and-hard Surfaces (SHS) ," *Electronic Components and Technology Conf. (ECTC)*, 27-30 May 2003, pp. 474-477.

[17] J. Ghalibafan, A. R. Attari, F. H. Kashani, "A New Dual-band Microstrip Antenna with U-shaped Slot," *Prog. in Electromagnetics Research C*, vol. 12, pp. 215-223, 2010.